CHEMISTRY
A EUROPEAN JOURNAL

DOI: 10.1002/chem.200701411

Self-Assembly of N^2-Modified Guanosine Derivatives: Formation of Discrete G-Octamers

Sanela Martić, Xiangyang Liu, Suning Wang,* and Gang Wu*[a]

Abstract: In the presence of Na^+ ions, two N^2-modified guanosine derivatives, N^2-(4-*n*-butylphenyl)-2′,3′,5′-*O*-triacetylguanosine (**G1**) and N^2-(4-pyrenylphenyl)-2′,3′,5′-*O*-triacetylguanosine (**G2**), are found to self-associate into discrete octamers that contain two G-quartets and a central ion. In each octamer, all eight guanosine molecules are in a *syn* conformation and the two G-quartets are stacked in a tail-to-tail fashion. On the basis of NMR spectroscopic evidence, we hypothesize that the π–π-stacking interaction between the N^2-side arms (phenyl in **G1** and pyrenyl in **G2**) can considerably stabilize the octamer structure. For **G1**, we have used NMR spectroscopic saturation-transfer experiments to monitor the kinetic ligand exchange process between monomers and octamers in CD_3CN. The results show that the activation energy (E_a) of the ligand exchange process is $31 \pm 5\ kJ\,mol^{-1}$. An Eyring analysis of the saturation transfer data yields the enthalpy and entropy of activation for the transition state: $\Delta H^{\neq} = 29 \pm 5\ kJ\,mol^{-1}$ and $\Delta S^{\neq} = -151 \pm 10\ J\,mol^{-1}\,K^{-1}$. These results are consistent with an associative mechanism for ligand exchange.

Keywords: guanosine · NMR spectroscopy · saturation transfer · self-assembly · supramolecular chemistry

Introduction

Molecular self-assembly via non-covalent interactions such as hydrogen bonding can lead to stable supramolecular structures. Hydrogen bonding between complementary DNA bases is one remarkable example of molecular self-assembly in nature. Among nucleobases, guanine exhibits the most versatile hydrogen-bonding capability; this results in a variety of self-assembled structures, such as dimers, trimers, G-ribbons and G-quartets.[1–3] In the past decade, the G-quartet structural motif has attracted considerable attention because of its biological implications.[4] In the meantime, applications of guanosine-based molecules in materials science and nanotechnology have also appeared.[5,6]

There are many factors that contribute to the overall structure of a G-quartet-based supramolecular entity. At the core of the G-quartet motif, non-covalent interactions, such as hydrogen-bonding and cation–dipole interactions, are the most important ones. Further stacking of G-quartets into octamers, dodecamers, hexadecamers, and even longer molecular cylinders depends on π stacking between bases, the sugar conformation, the glycosyl torsion angle (*syn* and *anti*), the type of templating cations (sometimes anions as well), protecting groups and other substitutions on the base that might provide additional attraction or hindrance. In general, guanosine-based derivatives with well-defined structure, stability and tuneable electronic, photonic, and magnetic properties are highly desirable.

For guanosine and 2′-deoxyguanosine derivatives, there are several potential points for modification that would not interfere with G-quartet formation: 2′, 3′, and 5′ positions of the ribose and C^8, N^2, and N^3 of the guanine base. To date, only C^8 and N^2 base modification has been utilized for G-quartet formation.[7–17] In many cases, base modification introduces new properties and flexibilities that might not be possible for the unmodified guanine. For example, Sessler and co-workers[6] reported that a C^8-modified guanosine nucleoside forms a G-quartet in the absence of templating metal ions, that is, it forms an "empty" G-quartet. Gottarelli, Spada, and co-workers[8,9] found that 8-oxoguanosines self-assemble into helical architectures. Kaucher and Davis[16] reported that N^2,C^8-disubstituted guanosine derivatives can form G-quartets. We recently demonstrated that a N^2-modified guanosine derivate can form discrete G-octamers.[17] It is anticipated that base modification can be used as a new handle in the design of new self-assembled guanosine struc-

[a] S. Martić, Dr. X. Liu, Prof. Dr. S. Wang, Prof. Dr. G. Wu
Department of Chemistry, Queen's University
90 Bader Lane, Kingston, Ontario K7L 3N6 (Canada)
Fax: (+1) 613-533-6669
E-mail: suning.wang@chem.queensu.ca
gang.wu@chem.queensu.ca

Supporting information for this article is available on the WWW under http://www.chemeurj.org/ or from the author.

tures. We report in this study the self-assembly of two N^2-modified guanosine nucleosides, N^2-(4-*n*-butylphenyl)-2′,3′,5′-*O*-triacetylguanosine (**G1**) and N^2-(4-pyrenylphenyl)-2′,3′,5′-*O*-triacetylguanosine (**G2**). A brief account on the

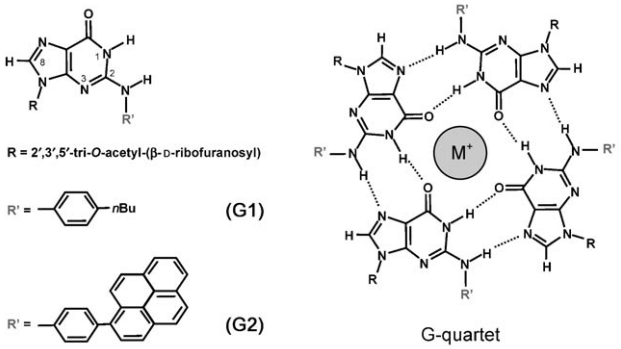

self-assembly of **G1** has been reported.[17] Here we report a detailed examination of the self-assembled structures that are formed by **G1** and **G2**, and of the kinetic ligand exchange between **G1** monomers and aggregates in solution.

Results and Discussion

Synthesis: The N^2-functionalized molecule, N^2-(4-*n*-butylphenyl)-2′,3′,5′-*O*-triacetylguanosine (**G1**) was synthesized by using a previously reported method.[18] The synthetic route to N^2-(4-pyrenylphenyl)-2′,3′,5′-*O*-triacetylguanosine) **G2** is shown in Scheme 1. Typically, Pd-catalyzed C–N bond coupling reactions are performed by using halogenated nucleosides or aryl halides; however, such methodology requires protection of the hydroxyl groups of the ribose moiety as well as the protection and subsequent deprotection of the O^6 site.[19] Our procedure is based on the well-known Ullmann condensation reactions, which are commonly used for the C–N coupling of aryl halides with aryl amines,[20,21] but have not been attempted with nucleosides previously. The starting material, *p*-pyrenyliodophenyl (**1**) was synthesized by lithiating 1-bromopyrene first, then by transmetalation to form a Zn^{II} complex and its cross coupling to *p*-diiodobenzene in the presence of $[Pd(PPh_3)_4]$ at 0 °C to give *p*-pyrenyliodophenyl (**1**) in 59% yield. Compound **2** was synthesized through an Ullmann condensation by using CuI as the catalyst and Cs_2CO_3 as the base at 140 °C. Protection of compound **2** was achieved by using an acetylation reaction with acetic anhydride in the presence of triethylamine and *N*-dimethylaminopyridine (DMAP) as a catalyst to give **G2** (see Scheme 1).

^{1}H NOESY NMR spectra: Figure 1 shows the spectral regions of the ^{1}H NOESY NMR spectra of **G1** and **G2** self-assemblies that were prepared in the presence of Na^+ ions. The observed interbase NOE cross peaks between H_8 and N_2H protons are characteristic features that indicate G-quartet formation. In addition, strong NOE cross peaks are observed between H_8 and $H_{1'}$ for both **G1** and **G2** self-assemblies, which suggests that all **G1** and **G2** molecules are exclusively in a *syn* conformation. The observed NOE cross peaks between H_{ortho}/H_{meta} and $H_2/H_{3'}$ protons further support a *syn* conformation of the glycosidic bond so that the N^2-subtituent is approximately above the ribose ring. The crystal structure of the **G1** monomer also exhibits a *syn* conformation with a glycosyl torsion angle χ_{CN} (O4′-C1′-N9-C4)

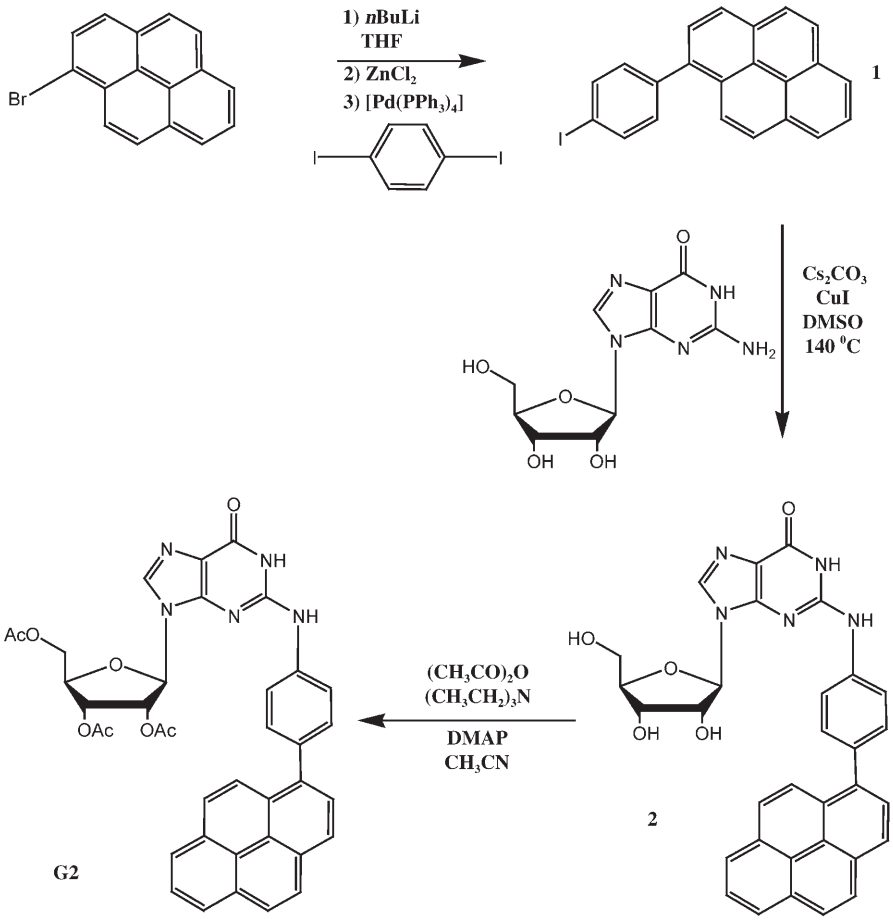

Scheme 1. Synthetic route to **G2**.

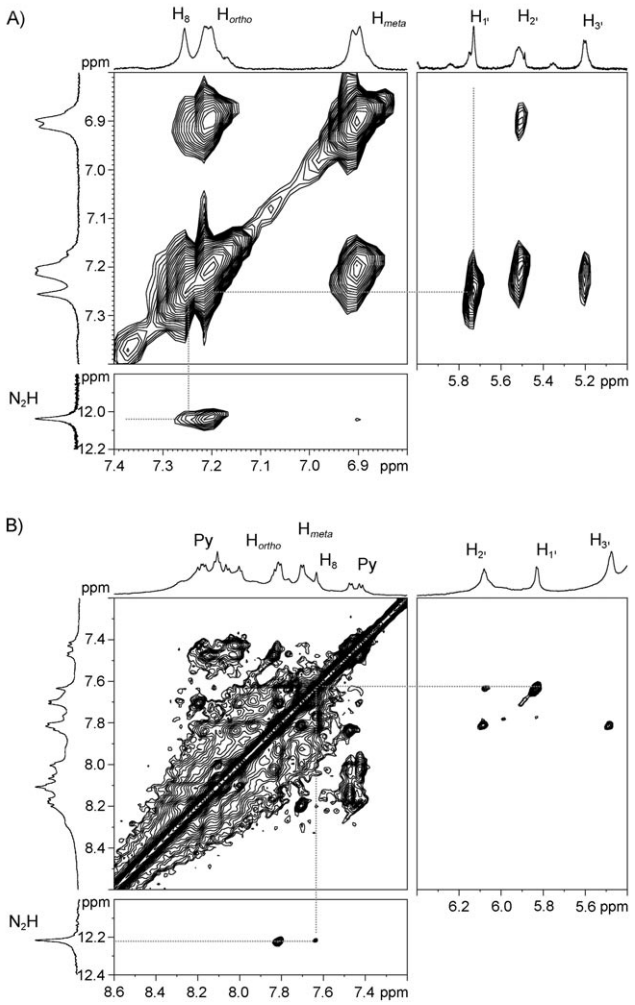

Figure 1. Regions of the NOESY spectra of A) **G1** in $CDCl_3$ and B) **G2** in CD_2Cl_2.

of 75.7°.[17] Our observation falls into the general trend that N^2 and C^8-modified guanosine derivatives usually prefer to adopt a *syn* conformation.[7,17,22] Also seen in Figure 1 are the strong NOE cross peaks between H_{ortho} and N_2H protons for both **G1** and **G2**, which are due to intrabase interactions. The fact that a single set of ^1H NMR signals for each octamer are observed suggests that the **G1** and **G2** octamers are D_4-symmetric.

The self-assembly process of both **G1** and **G2** appears to be rather sensitive to the solvent. For example, **G1** exists as monomers in CD_2Cl_2, as a monomer–aggregate mixture in CD_3CN, and exclusively as aggregates in $CDCl_3$. **G2** exists as monomers in $CDCl_3$, CD_3CN, and [D_6]acetone, and as aggregates only in CD_2Cl_2. At this time we do not have a satisfactory explanation for the observed solvent-dependence effect. The ^{23}Na NMR spectrum of the **G1** self-assembly in $CDCl_3$ exhibits a single peak at $\delta = -17.8$ ppm; this is in agreement with a G-octamer structure that contains a central Na^+ ion.[23–25] The ESI-MS spectra also suggest the presence of **G1** octamers. It is interesting to note that neither **G1** dodecamers nor **G1** hexadecamers were observed in the ESI-MS spectra, which is different from previous observations that have been made for other guanosine derivatives, for which polymeric aggregates are always likely to form in the presence of Na^+ or K^+ ions.[17,26,27] In addition, individual **G1** or **G2** tetramers were not observed either in the solution or gas phase. Perhaps, the particular stacking scheme between the two all-*syn* G-quartets in each **G1** octamer and the presence of acetyl protecting groups impose steric hindrance that prevents the stacking of two **G1** ocamers together. As will be discussed later, our models provide indirect evidence that supports this argument. The circular dichroism (CD) spectrum of **G1** in CH_3CN exhibits a nearly degenerate negative exciton couplet that is centered at 290 nm; this is similar to that reported for a G-octamer by Davis and co-workers.[27] This CD spectral feature is indicative of the twisted stacking of two chiral G-quartets.[28,29]

DOSY NMR spectroscopy: As mentioned in the previous section, NOESY data provide unambiguous evidence that **G1** and **G2** self-assemblies are based on the G-quartet structural unit. On the other hand, the ESI-MS data support the presence of G octamers rather than dodecamers and hexadecamers in the gas phase. However, none of these techniques can answer the question as to the exact size of molecular aggregates in solution. To determine the precise size of molecular self-assemblies from **G1** and **G2** in solution, we used an NMR technique known as diffusion-ordered spectroscopy (DOSY).[30,31] In general, a DOSY spectroscopic experiment measures the translational diffusion coefficient (D) of a molecule, which can then be used to infer the exact size of the molecule or molecular aggregate in solution. Recently, DOSY or diffusion NMR spectroscopy has been extensively used in supramolecular chemistry.[27,32–40] Experimental results of translational diffusion constants for **G1** and **G2** in various solvents are given in Table 1. We have also measured the value of D for the unmodified 2′,3′,5′-*O*-triacetylguanosine (TAG) in DMSO. Because TAG exists as

Table 1. Translational diffusion coefficients (in units of 10^{-10} m^2s) determined for TAG monomer, **G1** monomer, **G2** monomer, **G1** octamer, and **G2** octamer in different solvents. All NMR diffusion measurements were performed at 298 K.

	TAG[a]	G1			G2		
Solvent viscosity (η)[c]	$D_{monomer}$	$D_{monomer}$	D_8	$D_8/D_{monomer}$	$D_{monomer}$	D_8	$D_8/D_{monomer}$
DMSO (2.001)	1.44	–	-	–	–	-	–
$CDCl_3$ (0.542)	5.32[b]	6.06	3.09	0.51	–	–	–
CD_3CN (0.345)	8.35[b]	9.28	4.76	0.51	–	–	–
CD_2Cl_2 (0.432)	6.67[b]	–	–	–	8.14[b]	4.17	0.51
CD_3COCD_3 (0.307)	9.38[b]	–	–	–	11.2	5.56[b]	0.49

[a] TAG = 2′,3′,5′-*O*-triacetylguanosine [b] Calculated by using the relationship between solvent viscosity and *D*. [c] Solvent viscosity data at 298 K in units of cP.

monomers in DMSO, the experimental D value for TAG was used as an independent reference for G monomers. For easy comparison, we have calculated the expected D values for TAG in other solvents by using the inverse dependence between D and the solvent viscosity (η). As seen from Table 1, the value of D for **G1** monomers in $CDCl_3$, which was prepared in the absence of Na^+ ions is $6.06 \pm 0.05 \times 10^{-10}\,m^2s$. This value is approximately 14% larger than that of TAG in the same solvent, $5.32 \times 10^{-10}\,m^2s$. This suggests that the N^2 modification of **G1** also plays a role in the overall shape of the molecule compared to that of the unmodified guanosine. For **G1** and **G2** monomers in other solvents, the values of D are generally larger than the corresponding values of TAG by approximately 20%. When Na^+ ions are present in the solution, **G1** self-associates into aggregates and has a much smaller D value of $3.09 \times 10^{-10}\,m^2s$. The ratio between the two D values for **G1** monomers and **G1** aggregates suggests that **G1** molecules form octamers in $CDCl_3$.[22] As seen from Table 1, the values of D for **G2** aggregates also suggest the formation of **G2** octamers.

The most interesting case is that of **G1** in CD_3CN. The ^1H NMR spectrum of **G1** in CD_3CN that was prepared in the presence of Na^+ ions generally exhibits two sets of NMR signals. Furthermore, the two sets of signals exhibit quite different D values: 4.76 and $9.28 \times 10^{-10}\,m^2s$. Once again, the diffusion data immediately suggest that **G1** exists as a mixture of monomers and octamers in CD_3CN. This situation is best illustrated in the 2D representation of the DOSY data that is shown in Figure 2. In a sense, DOSY spectroscopy is a type of NMR chromatography that separates molecular species according to their translational mobility. Another interesting observation is that the NOE cross peaks that are due to **G1** monomers and **G1** octamers have opposite signs; this is illustrated in Figure 2, and can be understood on the basis that **G1** monomers and **G1** octamers have very different rotational correlation times (τ_C). It is well known that for small molecules in which τ_C is short relative to $1/\omega_0$ (ω_0 is the angular Larmor frequency of the nucleus under observation), the NOE cross peaks exhibit an opposite sign to the diagonal peaks. On the other hand, for large molecules or molecular aggregates with a long τ_C value relative to $1/\omega_0$, NOE cross peaks have the same sign as the diagonal peaks. In the present case, because **G1** octamers (ca. 4300 Da) are much larger than **G1** monomers (540 Da), they have quite different values of τ_C; this gives rise to NOE cross peaks with opposite signs. This observation, in turn, is in agreement with the diffusion NMR spectroscopic results. We have also found that the amount of **G1** octamers relative to that of **G1** monomers increases with a decrease of temperature, this indicates that the octamer formation is an exothermic process. Our dilution experiments of **G1** in CD_3CN also suggest that the octamer formation is favored at higher concentrations at 298 K, while a concentration effect is negligible at 283 K. **G2** exists exclusively as octamers in CD_2Cl_2 and as monomers in [D_6]acetone. We did not find any solvent in which **G2** exists as a mixture of monomers and octamers.

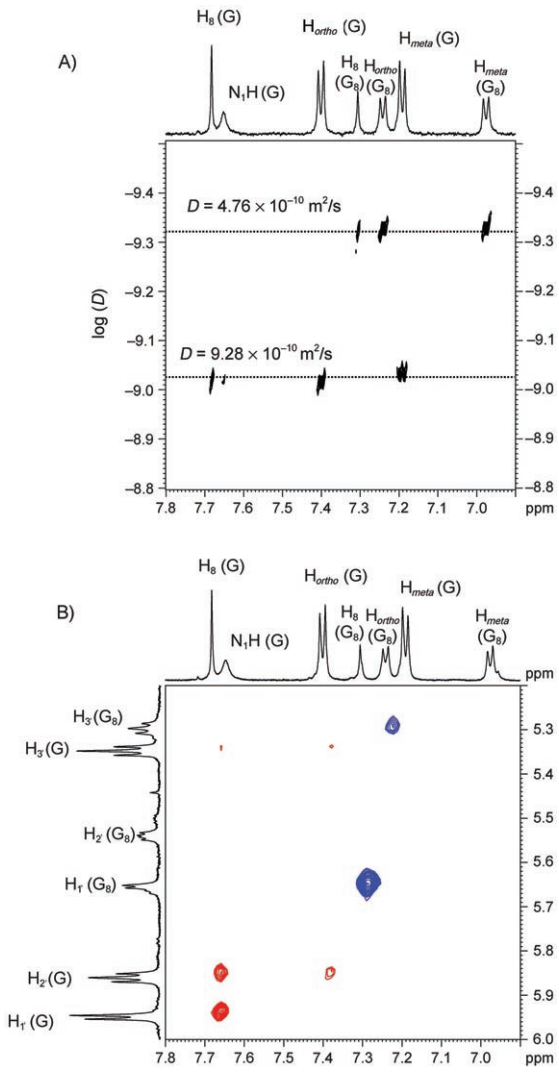

Figure 2. A) 2D representation of the DOSY data for **G1** in CD_3CN. B) A spectral region of the NOESY spectrum of **G1** in CD_3CN. The NOE cross peaks in blue and red have the same and opposite signs as the diagonal peaks, respectively.

Molecular structures of G1 and G2 octamers: Because crystallization of **G1** and **G2** octamers were unsuccessful, the model building in this section is based primarily on NMR spectroscopic evidence. As mentioned earlier, the ^1H NMR spectroscopic data suggest that **G1** and **G2** form D_4-symmetric octamers, each of which contains two all-*syn* G-quartets. As shown in Figure 3, the molecular structure of the **G1** monomer[17] exhibits a *syn* conformation with a glycosyl torsion angle of 75.7°. Another important structural feature of the **G1** monomer is that the five-membered ribose ring is puckered in the ^2E (2′-*endo*) conformation. We have therefore built a G octamer model by assuming a similar glycosyl torsion angle and sugar conformation. Because each G-quartet has two faces, head and tail, as illustrated in Figure 3, there are still two possible ways to form a D_4-symmetric octamer, that is, either head-to-head or tail-to-tail. Our model

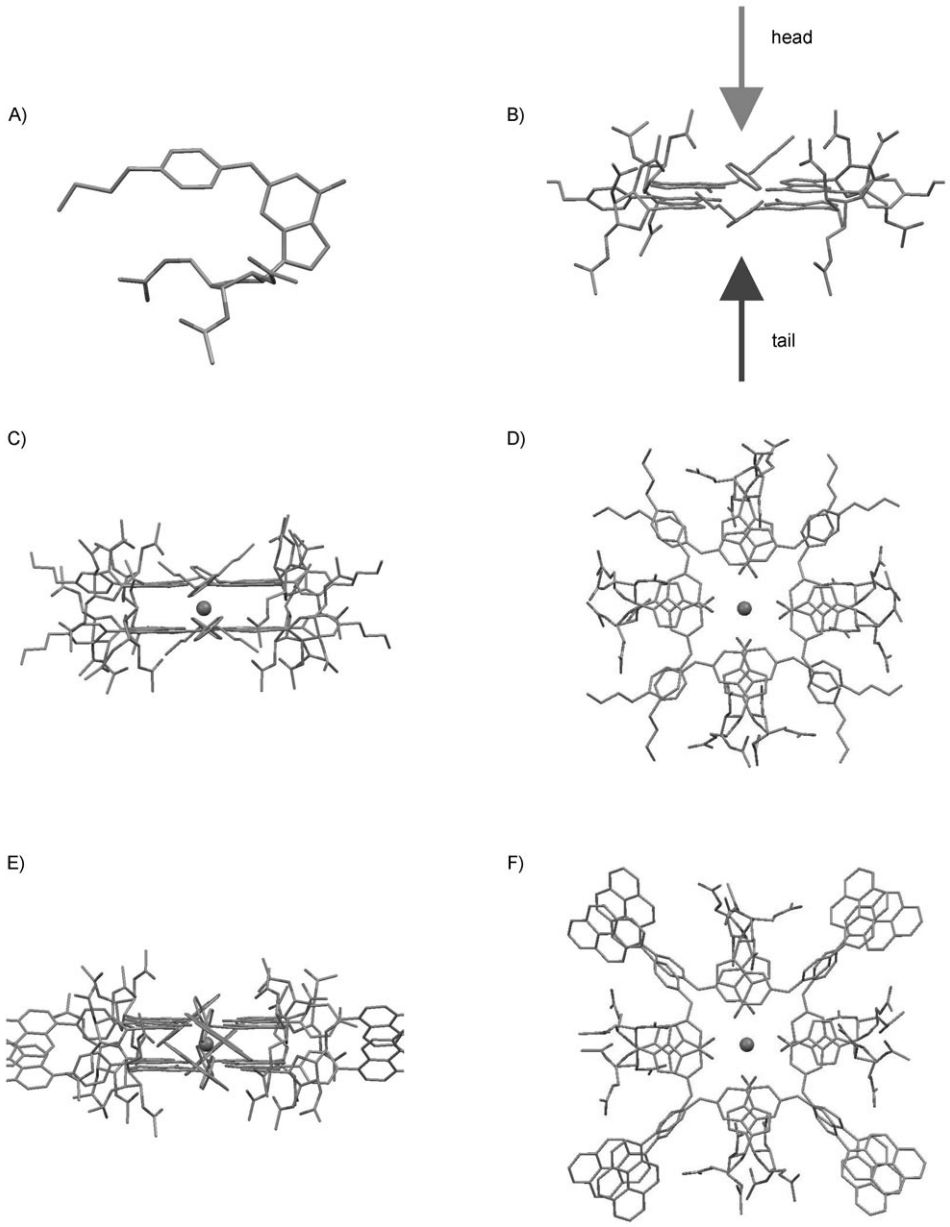

Figure 3. A) Crystal structure of the **G1** monomer. B) Illustration of the head and tail faces of a G-quartet. Top views (D and F) and side views (C and E) of the **G1** and **G2** octamers.

suggests that the tail-to-tail stacking is most likely to occur because of the arrangement of the three acetyl groups. In particular, as seen in Figure 3, the 2′- and 3′-*O*-acetyl groups are on the head side of the G-quartet and 5′-*O*-acetyl group is on the tail side. As a result, the head face is more crowded than the tail side. Furthermore, because of the additional methylene group that is linked to the 5′-*O*-acetyl group, it is more flexible than the 2′- and 3′-*O*-acetyl groups that are directly attached to the ribose ring. A tail-to-tail G-octamer formation can also provide an explanation for the fact that further stacking between octamers has not been observed for **G1** and **G2**.

The molecular models of the **G1** and **G2** octamers also suggest possible π–π-stacking interactions between the phenyl (**G1**) and pyrenyl (**G2**) aromatic rings from the two different G-quartets. Indeed, as seen from Figure 4, the observed ^{1}H NMR chemical shifts for the phenyl protons (H_{ortho} and H_{meta}) for the **G1** octamer are considerably more shielded than those in the **G1** monomer. In $CDCl_3$, such changes amount to $\Delta\delta = 0.34$ and 0.18 ppm for H_{ortho} and H_{meta}, respectively. In CD_3CN, we also found $\Delta\delta = 0.15$ and 0.20 ppm for H_{ortho} and H_{meta}, respectively. For **G2**, significant ^{1}H NMR chemical shift changes (ca. $\Delta\delta \approx 0.5$ ppm) were observed for H_7 and H_2 of the pyrenyl group. These chemical shift changes are comparable to those that were observed for the H_8 protons ($\Delta\delta = 0.42$ ppm for **G1** and $\Delta\delta = 0.45$ ppm for **G2**), which are due to the π–π stacking between the bases. Other protons of the pyrenyl group, even in the absence of a complete assignment, also show small chemical shift changes. All these observations are consistent with the formation of π–π stacking. Interestingly, the phenyl protons in the **G2** octamer exhibit little chemical shift change compared to those in the **G2** monomer. Inspection of the molecular model reveals that the phenyl rings in the **G2** octamer are more perpendicular to the guanine base plane than those in the **G1** octamer. In particular, the C^2-N^2-C_{ipso}-C_{ortho} torsion angle in the **G2** octamer is 78°, whereas it is only 41° in the **G1** octamer. Such an arrangement of the phenyl ring relative to the guanine plane was also predicted by quantum chemical calculations at the B3LYP/6–311+G(d) level for **G2** and from the crystal structure for the **G1** monomer. Consequently, there is very little π–π stacking between the two phenyl rings in the **G2** octamer. This is entirely consistent with the observation shown in Figure 4, in which the ^{1}H NMR signals for H_{ortho} and H_{meta} show little variations between **G2** monomers and **G2** octamers. On the other hand, significant ^{1}H NMR spectroscopic chemical shift changes are observed for H_{ortho} and H_{meta} protons between the **G1** monomer and **G1** octamer as mentioned earlier.

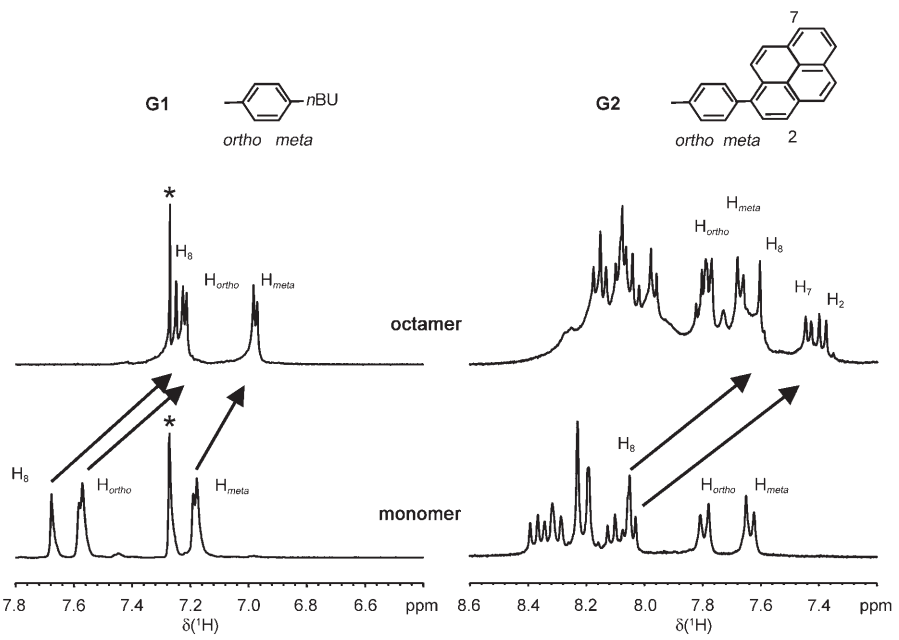

Figure 4. Regions of ^{1}H NMR spectra for **G1** in $CDCl_3$ (monomer and octamer) and **G2** in CD_2Cl_2 (octamer) and DMSO (monomer). * marks the solvent peak.

Another piece of evidence that suggests that there is π–π stacking between the pyrenyl rings in the **G2** octamer comes from the NOESY data. In the NOESY spectrum that is shown in Figure 5, cross peaks are observed between H_7 and H_2 of the pyrenyl group. As shown in Figure 5, the distance between H_2 and H_7 within the same pyrenyl ring is approximately 8.027 Å. This distance is generally too long to generate any NOE effect. On the other hand, the **G2** octamer model suggests that the distance between H_2 and H_7 from two different G-quartets (interquartet) is about 2.926 Å. This is a reasonable short contact for producing the observed NOE cross peaks. We have also measured the fluorescence spectra for **G2** in CH_2Cl_2. However, we did not observe a pyrene excimer peak. Presumably at the low concentrations that are suitable for the optical measurement, very little **G2** octamers are present.

In a G-octamer, the main forces to hold two G-quartets together are the ion–carbonyl interaction and the π–π stacking between the guanine bases. It is plausible that the additional π–π stacking between the N^2 side-arms in both **G1** and **G2** octamers further stabilizes these octamer structures. It would be interesting to design new N^2-modified guanosine derivatives in which the π–π stacking between the N^2 groups can be optimized. It might also be possible that such a π–π stacking between N^2 groups would provide a strong enough attraction to hold the two G-quartets so that the central cation becomes unnecessary, this would give rise to an "empty" G-octamer. Experiments to search for such an empty G-octamer are underway in our laboratory.

Ligand exchange between G1 monomers and octamers: As mentioned earlier, **G1** exists as a mixture of monomers and octamers in CD_3CN. This provides an excellent opportunity to examine ligand exchange between the free (monomers) and bound (octamers) states; see Scheme 2. However, variable temperature ^{1}H NMR spectra of **G1** do not exhibit any significant line broadening, which indicates that the ligand exchange rate is much slower than the NMR chemical shift time scale. For this reason, we employed a saturation transfer NMR spectroscopic technique to measure ligand exchange rates.[41,42] Typically, saturation transfer NMR experiments are performed by selectively saturating one NMR signal (signal A) from the **G1** monomer (or the octamer) and then monitoring the time evolution of the signal (signal B) from the **G1** octamer (or the monomer). According to Forsen and Hoffman,[41,42] the time evolu-

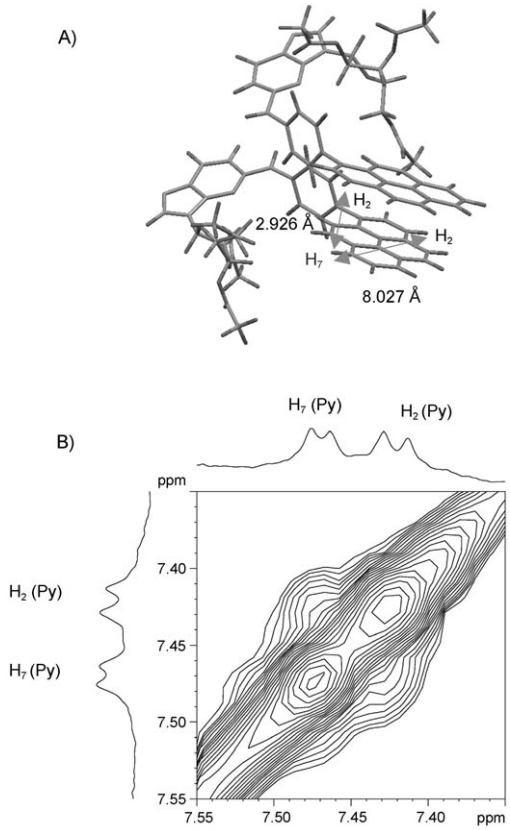

Figure 5. A) Part of the **G2** octamer model that shows the stacking between two pyrenyl groups. B) Expansion of the NOESY spectrum of **G2** octamers in CD_2Cl_2.

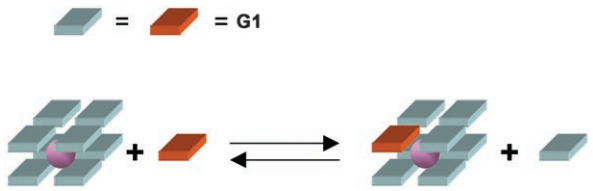

Scheme 2. Ligand exchange between **G1** monomers and octamers.

tion of signal A under the conditions of complete saturation of signal B can be written as:

$$\frac{M_z{}^A(t)}{M_O{}^A} = \frac{T_{1A}}{T_{1A}+\tau_A} e^{-\left(\frac{1}{\tau A}+\frac{1}{T1A}\right)t} + \frac{\tau_A}{T_{1A}+\tau_A}$$

in which T_{1A} is the spin–lattice relaxation time constant of signal A and τ_A is the lifetime of molecules in state A. The ligand exchange process between **G1** monomers and octamers is depicted in Figure 6. Because it is possible to find ^{1}H NMR spectral regions in which signals for both monomers and octamers are well resolved, we performed the saturation transfer experiments by saturating signals from monomers and octamers separately. Table 2 summarizes the saturation transfer NMR experimental results for **G1** in CD_3CN at different temperatures.

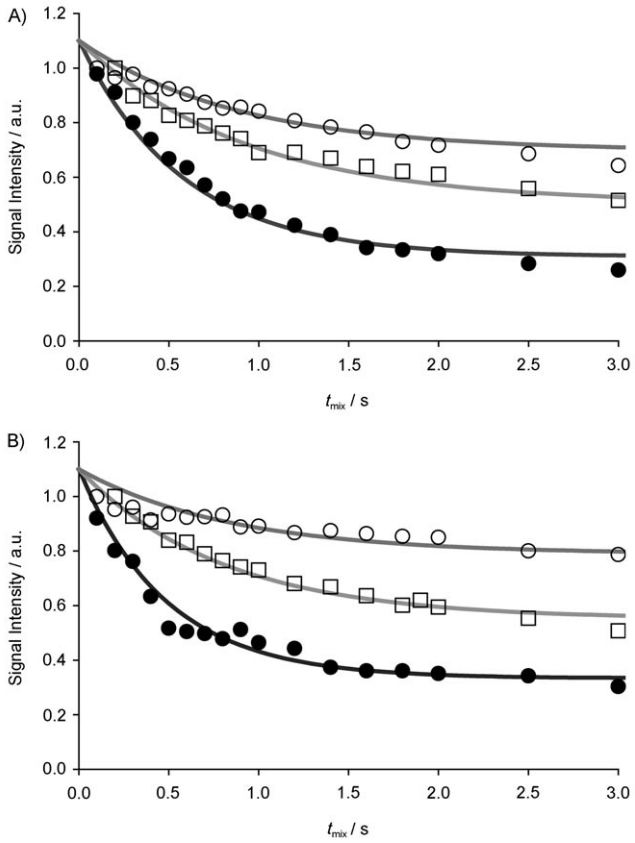

Figure 6. Saturation transfer NMR experiments for the **G1** ligand exchange in CD_3CN. A) Saturation of the NMR signal from octamers and B) saturation of the NMR signal from monomers. ○ 283 K; □ 298 K; ● 313 K.

Table 2. Saturation transfer NMR experimental results for **G1** kinetic ligand exchange in CD_3CN.

	Saturation of octamer signals			Saturation of monomer signals		
T [K]	T_{1A} [s]	τ_A [s]	$k=1/\tau_A$ [s^{-1}]	T_{1A} [s]	τ_A [s]	$k=1/\tau_A$ [s^{-1}]
283	1.39 (H8)	2.4±0.5	0.4	1.18 (H8)	3.0±0.5	0.3
298	2.01 (H1)	1.7±0.2	0.6	1.59 (H1)	1.6±0.2	0.6
313	2.05 (H8)	0.8±0.1	1.3	1.61 (H8)	0.7±0.1	1.4

The ligand exchange rates are in the order of a few s^{-1}. These values are comparable to those that were reported by Davis and co-workers for isoguanosines.[43] We also performed saturation transfer experiments for different concentrations, and the results suggest that ligand exchange rates decrease considerably at low concentrations. This is consistent with an associative bimolecular mechanism for the ligand exchange process.[44] An Arrhenius analysis of the data that is shown in Table 2 yields an activation energy (E_a) of 31 ±5 kJ mol^{-1} for the kinetic ligand exchange process. We have also applied an Eyring analysis for the saturation transfer data, and have obtained the enthalpy of activation and the entropy of activation for the transition state: $\Delta H^{\neq} = 29 \pm 5$ kJ mol^{-1} and $\Delta S^{\neq} = -151 \pm 10$ J mol^{-1} K^{-1}. Again, a large and negative value of $\Delta S^{\neq}$ is in agreement with the associative mechanism for ligand exchange.

Conclusion

We have shown that two N^2-modified guanosine derivatives form discrete G-octamers that contain all-*syn* guanosine molecules. The stacking between the two G-quartets is most likely in a tail-to-tail fashion. NMR spectroscopic results strongly suggest the formation of π–π stacking between the phenyl and pyrenyl groups in the **G1** and **G2** octamers, respectively. The kinetic ligand exchange between **G1** monomers and **G1** octamers is generally slow, and is in the order of a few s^{-1} between 283 and 313 K. We have determined the enthalpy and entropy of activation for the transition state: $\Delta H^{\neq} = 29 \pm 5$ kJ mol^{-1} and $\Delta S^{\neq} = -151 \pm 10$ J mol^{-1} K^{-1}. These data suggest an associative mechanism for the ligand exchange process. This study provides new insights into the self-assembly of N^2-modified guanosine compounds in organic solvents. It is quite clear that N^2-modification is a viable approach in the design of new G-quartet-based materials. Although this study deals with guanosine nucleosides, it is possible that the same strategy might be applicable to nucleotides (DNA and RNA) because the exocyclic amino N–H bond is pointing into the groove region. We believe that residue-specific N^2 modification should be exploited as a new handle for fine-tuning G-quadruplex structure and function.

Experimental Section

Synthesis details: All starting materials and reagents were purchased from Aldrich Chemical Company and were used without further purification. Thin-layer chromatography was carried out by using silica gel 60 plates, and the column chromatography was performed by using silica gel of particle size 60–200 μm and C-18 silica gel for reversed-phase chromatography, all of which were purchased from Silicycle. **G1** was synthesized by using a previously reported procedure.[17]

***p*-Pyrenyliodophenyl (1)**: A 1.6 M hexane solution of *n*BuLi (1.75 mL, 2.79 mmol) was added to a stirred solution of bromopyrene (0.71 g, 2.54 mmol) in THF (100 mL)at −78 °C. After 1 h at this temperature, $ZnCl_2$ (0.41 g, 3.04 mmol) was added and stirring was continued for 0.5 h at 0 °C. Diiodobenzene (1.81 g, 5.4 mmol) and $[Pd(PPh_3)_4]$ (0.22 g, 9 mol %) were added to the mixture, and the reaction was allowed to warm up to room temperature, and was stirred overnight under N_2. The solution was partitioned by using ethyl acetate (100 mL) and water (100 mL). The aqueous layer was further extracted with dichloromethane (3×40 mL), and the combined organic fractions were dried over anhydrous $MgSO_4$ and concentrated under vacuum. The product was purified by using column chromatography (hexane/ethyl acetate 5:1) and was isolated as a white solid. Yield: 0.610 g (59.4 %). ^{1}H NMR (400 MHz, $CDCl_3$, 25 °C): δ = 8.24–7.94 (m, J = 3.6, 7.8, 9.2 Hz, 9H), 7.91 (d, J = 8.3 Hz, 2H, H_{ortho}), 7.39 ppm (d, J = 8.3 Hz, 2H, H_{meta}); ^{13}C NMR (400 MHz, $CDCl_3$, 25 °C): δ = 140.7, 137.5, 136.4, 132.5, 131.5, 131.2, 130.9, 130.8, 128.3, 128.1, 127.7, 127.6, 127.4, 127.3, 126.1, 125.8, 125.3, 125.0, 124.9, 124.8, 124.6, 93.1 ppm; HRMS (EI+): *m*/*z*: calcd for $C_{22}H_{13}I$: 404.0062; found: 404.0046 $[M]^+$.

N^2-(4-Pyrenylphenyl)guanosine (2): A mixture of *p*-pyrenyliodophenyl (0.199 g, 0.49 mmol), guanosine (0.209 g, 0.73 mmol), cesium carbonate (0.192 g, 0.59 mmol), copper iodide (0.014 g, 0.07 mmol, 15 %), and DMSO (5 mL) in small sealable 25 mL vial was degassed with N_2 for 10 min, then the vial was sealed, and the reaction was carried out at 140 °C for 24 h in a preheated oil bath. Water (10 mL) was added to reaction mixture, and the solution was neutralized to pH ≈ 7 by using aq. HCl. Further addition of water (30 mL) led to the precipitation of the product as a beige solid. The solid was washed with water to remove unreacted guanosine, then it was purified by using reversed-phase silica (CH_2Cl_2, then MeOH/H_2O 4:1) to obtain N^2-(4-pyrenylphenyl) guanosine (0.061 g, 22.3 %) as a white solid. ^{1}H NMR (400 MHz, [D$_6$]DMSO, 25 °C): δ = 10.76 (brs, 1H; N^{1}H), 9.14 (brs, 1H; N^{2}H), 8.4–8.26 (m, 3H), 8.21 (d, J = 9.17 Hz, 4H), 8.11 (s, 1H, H^8), 8.06 (t, J = 8.01 Hz, 2H), 7.86 (d, J = 8.28 Hz, 2H; H_{ortho}), 7.64 (d, J = 8.21 Hz, 2H; H_{meta}), 5.83 (d, J = 5.46 Hz, 1H; $H_{1'}$), 5.53 (d, J = 5.94 Hz; C_2-OH), 5.21 (d, J = 5.12 Hz; C_3-OH), 5.02 (t, J = 5.16, 5.35 Hz; C_5-OH), 4.55 (q, J = 5.33, 5.68 Hz, 1H; $H_{2'}$), 4.13 (d, J = 4.33 Hz, 1H; $H_{3'}$), 3.90 (d, J = 3.52 Hz, 1H; $H_{4'}$), 3.55 ppm (m, J = 4.06, 6.78, 14.78 Hz, 2H; $H_{5'}$, $H_{5''}$); ^{13}C NMR (400 MHz, [D$_6$]DMSO, 25 °C): δ = 157.7, 150.9, 150.5, 138.9, 137.9, 132.1 (2C), 131.9 (2C), 131.5, 131.1, 128.8 (2C), 128.7 (2C), 128.5 (2C), 127.6, 126.4, 126.1 (2C), 125.4, 125.3, 125.2, 123.8, 121.4 (2C), 120.2, 86.9 (C_1), 79.5 (C_4), 72.3 (C_2), 70.4 (C_3), 63.3 ppm (C_5); HRMS (ESI+): *m*/*z*: calcd for $C_{32}H_{25}N_5O_5$: 560.1934; found: 560.1943 $[M+H]^+$.

N^2-(4-Pyrenylphenyl)-2′,3′,5′-O-triacetylguanosine (G2): Acetic anhydride (0.094 mL, 0.98 mmol) was added to a suspension of N^2-(4-pyrenylphenyl) guanosine (0.041 g, 0.07 mmol) and *N*-dimethylaminopyridine (0.003 g, 0.02 mmol) in a mixture of acetonitrile (6 mL) and triethylamine (0.151 mL, 1.08 mmol) at room temperature. After stirring for 1 h, when all of the starting material had dissolved, MeOH (5 mL) was added to the mixture, and stirring was continued for an additional 5 min. The solution was then evaporated to dryness, and the resulting oil was precipitated out with *i*PrOH. The solid was isolated by centrifugation and was washed with diethyl ether. The solid was dissolved in THF and the compound was purified by preparatory TLC (MeOH/CH_2Cl_2, 1:9 (*v*/*v*) and MeOH/ethyl acetate 1:9 (*v*/*v*)). After extensive purification, a white product (15 mg, 31.8 %) was isolated. ^{1}H NMR (400 MHz, [D$_6$]DMSO, 25 °C): δ = 10.93 (brs, 1H; N^{1}H), 9.17 (brs, 1H; N^{2}H), 8.39–8.03 (m, J = 3.12, 4.22, 8.27 Hz, 10H; 9H pyrene, H_8), 7.78 (d, J = 8.38 Hz, 2H; H_{ortho}), 7.63 (d, J = 8.41 Hz, 2H; H_{meta}), 6.13 (d, J = 5.12 Hz, 1H; $H_{2'}$), 6.08 (t, J = 5.82 Hz, 1H; $H_{1'}$), 5.45 (t, J = 5.40 Hz, 1H; $H_{3'}$), 4.31 (m, J = 3.43, 4.02 Hz, 1H; $H_{4'}$), 4.28 (m, J = 4.6, 6.1, 10.1 Hz, 1H; $H_{5''}$), 4.15 (m, J = 4.8, 6.1, 10.2 Hz, 1H; $H_{5'}$), 2.06 (s, 3H; CH_3), 2.02 (s, 3H; CH_3), 1.86 ppm (s, 3H; CH_3); ^{13}C NMR (400 MHz, [D$_6$]DMSO, 25 °C): δ = 171.7, 170.2, 170.1, 157.3, 150.5, 150.2, 138.8, 137.6, 135.7, 131.8, 131.6 (2C), 131.2, 130.7, 128.4 (2C), 128.3 (2C), 128.2 (2C), 127.2, 126.1, 125.8, 125.7 (2C), 125.4, 125.0, 124.9, 121.1 (2C), 87.3 (C_1), 79.9 (C_4), 72.6 (C_2), 70.8 (C_3), 63.6 (C_5), 21.3 (CH_3), 21.0 (CH_3), 20.8 ppm (CH_3); HRMS (ESI+): *m*/*z*: calcd for $C_{38}H_{31}N_5O_8$: 686.2508; found: 686.22760 $[M+H]^+$.

NMR spectroscopic experiments: All routine ^{1}H and ^{13}C NMR spectra were recorded on Bruker Avance-500 and Avance-600 spectrometers. For **G1** octamers in $CDCl_3$, the source of Na^+ ions was either $NaClO_4$ or sodium picrate. For **G1** octamers in CD_3CN and **G2** octamers in CD_2Cl_2, no additional Na^+ ions were added to the samples because Na^+ ions had apparently been extracted into the samples during the compound synthesis and NMR sample preparation. Although at that time, the exact source of Na^+ and the nature of counter ions were uncertain, the presence of the Na^+ ions in these samples was unambiguously proved by solution ^{23}Na NMR and cryptand extraction experiments.

Pulse field gradient (PEG) NMR spectroscopy: Diffusion experiments were carried out with Bruker Avance-600 MHz spectrometer by using the pulse sequence of longitudinal-eddy-current delay (LED) with bipolar-gradient pulses. The ^{1}H 90° and 180° pulse widths were 10 and 20 μs, respectively. The pulse-filed gradient duration was varied from 4–15 ms, and the variable gradient (G) was changed from 6 to 350 mT/m. The diffusion period was varied from 50 to 90 ms. A total of 16 transients were collected for each of the 32 increment steps with a recycling delay 12 s. The eddy-current delay was set to 5 μs. Diffusion coefficients were obtained by integration of the desired peaks to a single exponential decay curve by using "Simfit Bruker XWINNMR" software. Calibration of the field gradient strength was achieved by measuring the value of translational diffusion coefficient (D) for the residual ^{1}H signal in D_2O (99.99 %, ^{2}H atom), $D = 1.91\times10^{-9}$ m^2 s.

NOESY spectroscopy: All NOESY spectra at 298 K were acquired by using a mixing time of 0.4 s and a total of 64 transients with a recycling delay of 10 s. The NOESY experiment at 218 K was acquired by using a mixing time of 0.1 s and a recycling delay of 2 s and a total of 64 transients.

Saturation transfer experiments: Selective saturation transfer experiments were performed for **G1** in CD_3CN between 283 and 313 K. The experiments were conducted by using a selective saturation pulse on the peak of interest. An irradiation at H_8 of the **G1** monomer or $(\mathbf{G1})_8$ octamer was used at 283 and 313 K, while irradiation at $H_{1'}$ of the **G1** monomer or $(\mathbf{G1})_8$ octamer was performed at 298 K. The spectra were collected by varying the mixing time from 0 to 14 s for a total of 24 data points. Each ^{1}H NMR spectrum was acquired by using 32 scans.

Mass spectrometry: ESIMS experiments were performed by using the positive-ionization mode on QSTA XL MS/MS systems by using the Analyst QS Method or on Waters Micromass ZQ Spectra were acquired over a *m*/*z* range of 100–10000. MALDI-TOF experiments were performed on the Voyager AB Applied Biosystems.

Circular dichroism (CD) spectroscopy: CD spectra of **G1** and **G2** solutions were recorded on a Jasco 715 circular dichroism spectrometer in a 0.1 cm path length cuvette. The wavelength was varied from 190 to 800 nm at 1000 nm per min with 10 overall scans. The concentration of the **G1** solution was 250 μM and that of **G2** was 0.53 μM. The equilibrium CD curves were obtained in the 285–325 K range, and a suitable time (10 min) was used to achieve the equilibrium before recording CD.

Acknowledgement

This work was supported by NSERC of Canada. S.M. thanks the Province of Ontario for an Ontario Graduate Scholarship (2006-07).

[1] G. Gottarelli, G. P. Spada, *Chem. Rec.* **2004**, *4*, 39–49.
[2] S. Sivakova, S. J. Rowan, *Chem. Soc. Rev.* **2005**, *34*, 9–21.
[3] J. T. Davis, *Angew. Chem.* **2004**, *116*, 684–716; *Angew. Chem. Int. Ed.* **2004**, *43*, 668–698.
[4] *Quadruplex Nucleic Acids* (Eds.: S. Neidle, S. Balasubramanian), The Royal Society of Chemistry, Cambridge (UK), **2006**.
[5] J. T. Davis, G. P. Spada, *Chem. Soc. Rev.* **2007**, *36*, 296–313.
[6] A. B. Kotlyar, N. Borovok, T. Molotsky, H. Cohen, E. Shapir, D. Porath, *Adv. Mater.* **2005**, *17*, 1901–1905.
[7] J. L. Sessler, M. Sathiosatham, K. Doerr, V. Lynch, K. A. Abboud, *Angew. Chem.* **2000**, *112*, 1356–1359; *Angew. Chem. Int. Ed.* **2000**, *39*, 1300–1303.
[8] T. Giorgi, S. Lena, P. Mariani, M. A. Cremonini, S. Masiero, S. Pieraccini, J. P. Rabe, P. Samorì, G. P. Spada, G. Gottarelli, *J. Am. Chem. Soc.* **2003**, *125*, 14741–14749.
[9] S. Lena, M. A. Cremonini, F. Federiconi, G. Gottarelli, C. Graziano, L. Laghi, P. Mariani, S. Masiero, S. Pieraccini, G. P. Spada, *Chem. Eur. J.* **2007**, *13*, 3441–3449.
[10] V. Gubala, J. E. Betancourt, J. M. Rivera, *Org. Lett.* **2004**, *6*, 4735–4738.
[11] V. Esposito, A. Randazzo, G. Piccialli, L. Petraccone, C. Giancola, L. Mayol, *Org. Biomol. Chem.* **2004**, *2*, 313–318.
[12] A. Virgilio, V. Esposito, A. Randazzo, L. Mayol, A. Galeone, *Nucleic Acids Res.* **2005**, *33*, 6188–6195.
[13] G.-X. He, S. H. Krawczyk, S. Swaminathan, R. G. Shea, J. P. Dougherty, T. Terhorst, V. S. Law, L. C. Griffin, S. Coutre, N. Bischofberger, *J. Med. Chem.* **1998**, *41*, 2234–2242.
[14] M. Koizumi, K. Akahori, T. Ohmine, S. Tsutsumi, J. Sone, T. Kosaka, M. Kaneko, S. Kimura, K. Shimada, *Bioorg. Med. Chem. Lett.* **2000**, *10*, 2213–2216.
[15] T. Park, E. M. Todd, S. Nakashima, S. C. Zimmerman, *J. Am. Chem. Soc.* **2005**, *127*, 18133–18142.
[16] M. S. Kaucher, J. T. Davis, *Tetrahedron Lett.* **2006**, *47*, 6381–6384.
[17] X. Liu, I. C. M. Kwan, S. Wang, G. Wu, *Org. Lett.* **2006**, *8*, 3685–3688.
[18] G. E. Wright, L. W. Dudycz, *J. Med. Chem.* **1984**, *27*, 175–181.
[19] M. K. Lakshman, *J. Organomet. Chem.* **2002**, *653*, 234–251.
[20] F. Ullmann, J. Bielecki, *Chem. Ber.* **1901**, *34*, 2174–2185.
[21] J. Lindley, *Tetrahedron* **1984**, *40*, 1433–1456.
[22] D. B. Davies, *Progr. Nucl. Magn. Reson. Spectrosc.* **1978**, *12*, 135–225.
[23] G. Wu, A. Wong, *Chem. Commun.* **2001**, 2658–2659.
[24] A. Wong, J. C. Fettinger, S. L. Forman, J. T. Davis, G. Wu, *J. Am. Chem. Soc.* **2002**, *124*, 742–743.
[25] A. Wong, R. Ida, G. Wu, *Biochem. Biophys. Res. Commun.* **2005**, *337*, 363–366.
[26] I. Manet, L. Francini, S. Masiero, S. Pieraccini, G. P. Spada, G. Gottarelli, *Helv. Chim. Acta* **2001**, *84*, 2096–2107.
[27] M. S. Kaucher, Y.-F. Lam, S. Pieraccini, G. Gottarelli, J. T. Davis, *Chem. Eur. J.* **2005**, *11*, 164–173.
[28] S. L. Forman, J. C. Fettinger, S. Pieraccini, G. Gottarelli, J. T. Davis, *J. Am. Chem. Soc.* **2000**, *122*, 4060–4067.
[29] G. Gottarelli, S. Masiero, G. P. Spada, *Enantiomer* **1998**, *3*, 429–436.
[30] E. O. Stejskal, J. E. Tanner, *J. Chem. Phys.* **1965**, *42*, 288–292.
[31] D. Wu, A. Chen, C. S. Johnson, Jr., *J. Magn. Reson. Ser. A* **1995**, *115*, 123–126.
[32] A. Gafni, Y. Cohen, *J. Org. Chem.* **1997**, *62*, 120–125.
[33] L. Frish, F. Sansone, A. Casnati, R. Ungaro, Y. Cohen, *J. Org. Chem.* **2000**, *65*, 5026–5030.
[34] L. Avram, Y. Cohen, *J. Am. Chem. Soc.* **2002**, *124*, 15148–15149.
[35] L. Avram, Y. Cohen, *Org. Lett.* **2006**, *8*, 219–222.
[36] T. Megyes, H. Jude, T. Grosz, I. Bako, T. Radnai, G. Tarkanyi, G. Palinkas, P. J. Stang, *J. Am. Chem. Soc.* **2005**, *127*, 10731–10738.
[37] A. Wong, R. Ida, L. Spindler, G. Wu, *J. Am. Chem. Soc.* **2005**, *127*, 6990–6998.
[38] M. Tominaga, K. Suzuki, M. Kawano, T. Kusukawa, T. Ozeki, S. Sakamoto, K. Yamaguchi, M. Fujita, *Angew. Chem.* **2004**, *116*, 5739–5743; *Angew. Chem. Int. Ed.* **2004**, *43*, 5621–5625.
[39] M. S. Kaucher, W. A. Harrell, Jr., J. T. Davis, *J. Am. Chem. Soc.* **2006**, *128*, 38–39.
[40] T. Evan-Salem, L. Frish, F. W. B. van Leeuwen, D. N. Reinhoudt, W. Verboom, M. S. Kaucher, J. T. Davis, Y. Cohen, *Chem. Eur. J.* **2007**, *13*, 1969–1977.
[41] S. Forsen, R. A. Hoffman, *J. Chem. Phys.* **1963**, *39*, 2892–2901.
[42] S. Forsen, R. A. Hoffman, *J. Chem. Phys.* **1964**, *40*, 1189–1196.
[43] M. Cai, V. Sidorov, Y.-F. Lam, R. A. Flowers II, J. T. Davis, *Org. Lett.* **2000**, *2*, 1665–1668.
[44] K. M. Brière, C. Detellier, *J. Phys. Chem.* **1992**, *96*, 2185–2189.

Received: September 6, 2007
Published online: November 26, 2007

